Journal of Photochemistry and Photobiology A: Chemistry 221 (2011) 232–238

Contents lists available at ScienceDirect

Journal of Photochemistry and Photobiology A: Chemistry

journal homepage: www.elsevier.com/locate/jphotochem

Nano-patterning of a TiO_2-organic hybrid material using interference of surface plasmon on aluminum

Hiroyo Segawa*, Satoru Inoue, Minoru Osada, Yoshihiko Takeda

National Institute for Materials Science, 1-1 Namiki, Tsukuba 305-0044, Japan

ARTICLE INFO

Article history:
Available online 10 March 2011

Keywords:
Organic–inorganic hybrid materials
Interference
Surface plasmon
Nano-patterning
Ceramic

ABSTRACT

Nano patterns of a TiO_2-organic hybrid material have been fabricated by interference of surface plasmon on aluminum. The TiO_2-organic hybrid materials were prepared by the sol–gel method, and were irradiated through an aluminum mask by a UV light. After the unreacted parts were removed, patterns were obtained on the films. The patterns of lines approximately 300 nm in width and with a sub-100-nm height were obtained by controlling the UV irradiation time. It was confirmed that the patterns changed to anatase patterns by sintering at temperatures above 450 °C.

1. Introduction

Nanolithography has been developed to fabricate nanoscale devices. Many methods, including near-field optical lithography [1–3], electron-beam lithography [4], X-ray lithography [5], and imprint lithography [6] have been developed to achieve nanometer-scale features. Near-field optical lithography especially appears to have potential as a derivative technique of conventional photolithography because the pattern sizes are not restricted by the diffraction limit of light. In near-field optical lithography, the electric field enhanced by surface plasmon (SP), which is induced by noble metals with nanometer size, has more potential for high-efficiency techniques.

SP is known to interfere on the metal surface, and the electric field is enhanced with a nano scale distribution. Luo and Ishihara have reported that the interference of surface plasmon on silver patterns can be simulated by finite difference time domain (FDTD) calculations, and nano patterns of a photoresist were demonstrated experimentally by light irradiation of a wavelength of 436 nm [7].

Generally, most photoresists have good sensitivity in a short wavelength range such as 365 nm. The SP of aluminum (Al) is known to be oscillated at a shorter wavelength than that of silver or gold [8,9]. Recently, the SP of Al with nanometer size was demonstrated by calculations and experimental studies [10]. Srituravanich et al. have shown that the SP of Al was enhanced by UV light, and sub-100-nm dot arrays of a photoresist were demonstrated by contacting of an Al mask [11].

In contrast, in our previous work, patterns of a TiO_2-organic hybrid material were fabricated using UV irradiation [12], and another TiO_2-organic hybrid material was changed to anatase by sintering [13]. The hybrid materials were prepared by the sol–gel method from Ti alkoxide and β-diketone. The Ti alkoxide reacted with β-diketone, and chelate compounds were formed. The chelated compound was decomposed by the UV irradiation, and the unreacted parts of the hybrid films were dissolved in alcohol, resulting in patterns of micrometer size being fabricated.

As mentioned above, some hybrid films can be used to make patterns of ceramics or glasses by photolithography and sintering, although it is known to be more difficult to form patterns of ceramics or glasses than polymers due to the chemical stability. Thus, if the SP was used for the patterning of inorganic-organic hybrid materials, patterns with nanometer size might be made by the interference of SP and nano-patterns of ceramics or glasses could be fabricated by sintering of the hybrid materials.

In this study, the nano-patterning of negative-type TiO_2-organic hybrid materials by the interference on the SP of the Al was demonstrated, and TiO_2 nano patterns were obtained by sintering of the hybrid patterns.

2. Calculation details

Electric field distribution on the surface of Al was calculated by the FDTD method. Fig. 1(a) shows a schematic model for the calculations, which were carried by a two dimensional model. In the model, Al patterns were assumed to coat a silica glass, and were in contact with a hybrid film, for which the refractive index was set to 1.7, as in our previous work [12]. UV light with a wavelength of 365 nm was assumed as a light source. At first, the line

* Corresponding author. Tel.: +81 29 860 4601.
E-mail address: SEGAWA.Hiroyo@nims.go.jp (H. Segawa).

1010-6030/$ – see front matter © 2011 Elsevier B.V. All rights reserved.
doi:10.1016/j.jphotochem.2011.02.019

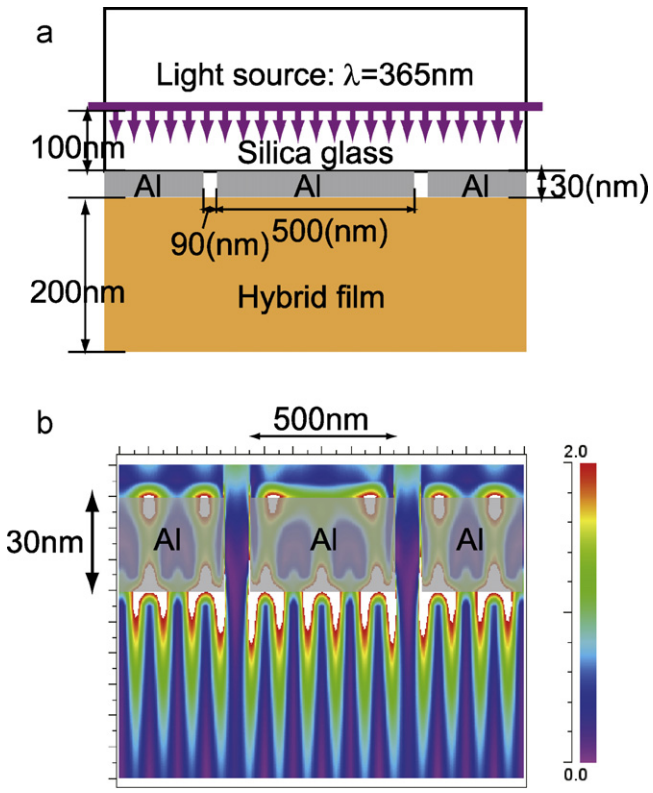

Fig. 1. FDTD calculation of near field on surfaces of Al: (a) schematic model and (b) obtained electric field distribution.

width of Al, the thickness of Al, and the gap size between neighboring Al were investigated. In the model, as shown in Fig. 1(a), the electric field was formed from interference distribution and was strongly enhanced. The calculated electric field is shown in Fig. 1(b). The enhancement of the Al edge was the strongest, and 4 points on the Al surface with 500 nm width were enhanced strongly due to interference of the plasmon. The distance between each enhanced distribution was approximately 100 nm. The enhancement of the interference distribution was the strongest in the region from the surface of Al to approximately 15 nm beneath the surface. The interference gradually weakened with increasing distance from the surface and was observed until the region approximately 50 nm beneath the Al surface.

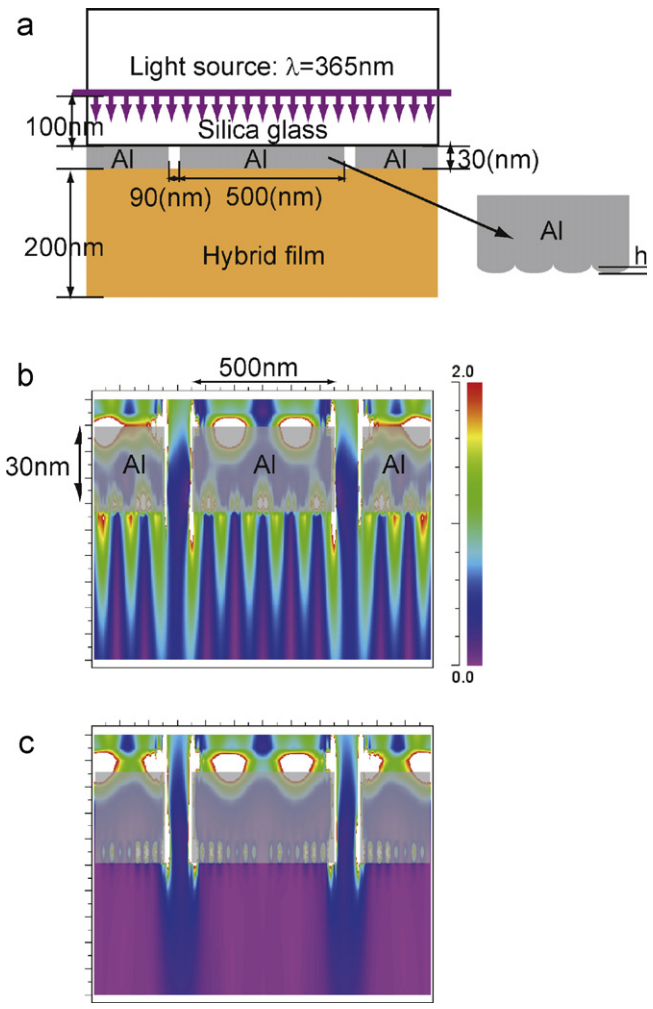

Fig. 2. FDTD calculation (a) for model to investigate the influence of the roughness of the Al surface, and obtained electric field distribution for the aluminum surface with roughness (b) $h = 2.7$ nm and (c) $h = 4.0$ nm.

Next, the influence of roughness on the Al surface was investigated by using the model shown in Fig. 2(a). Periodic roughness was inserted onto the surface of Al by convex surfaces with height, h. The calculated electric field distributions are shown in Fig. 2(b) and (c). When the height of the convex surfaces was 2.7 nm, the

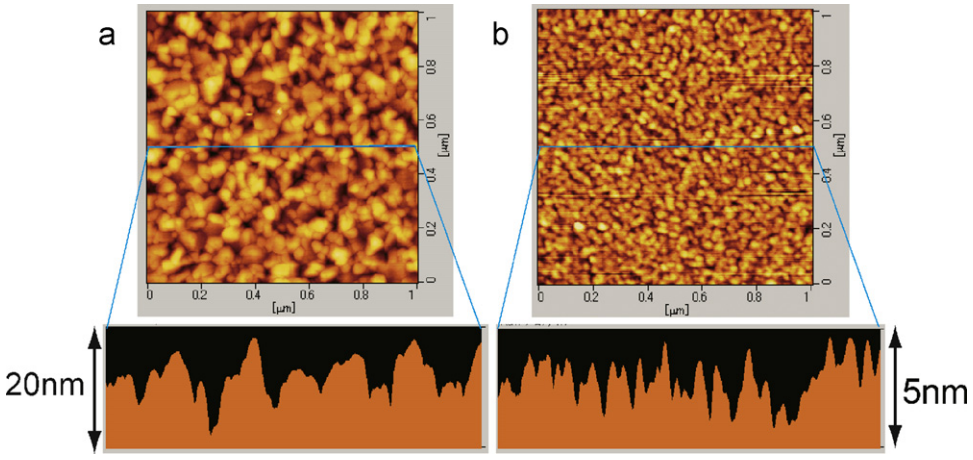

Fig. 3. AFM images of the aluminum surface of (a) Ra = 2.5 nm and (b) Ra = 0.59 nm.

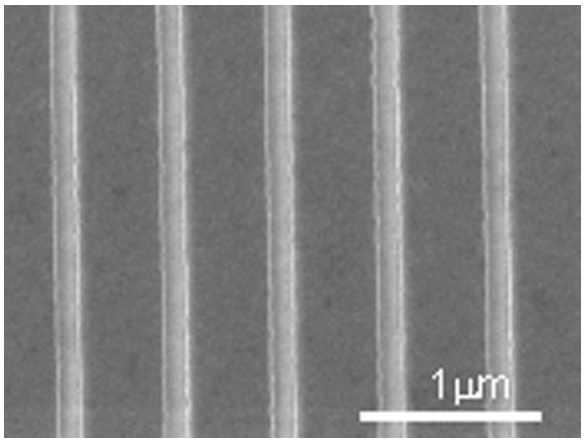

Fig. 4. An SEM image of the surface of patterned Al of mask B.

interference was observed as shown in Fig. 2(b). The enhancement by interference of the SP became weak with increases in the height of the convex surface. The interference of the electric field was not observed in the case of $h = 4.0$ nm, as shown in Fig. 2(c). This means that it is important to control the roughness of the Al surface to create the interference of the SP.

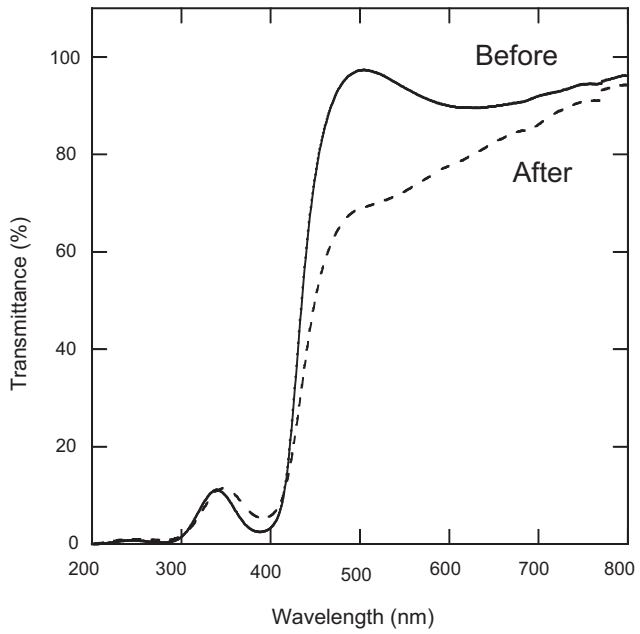

Fig. 6. UV–vis transmittance spectra of the TiO_2-organic hybrid film before and after UV irradiation for 5 min.

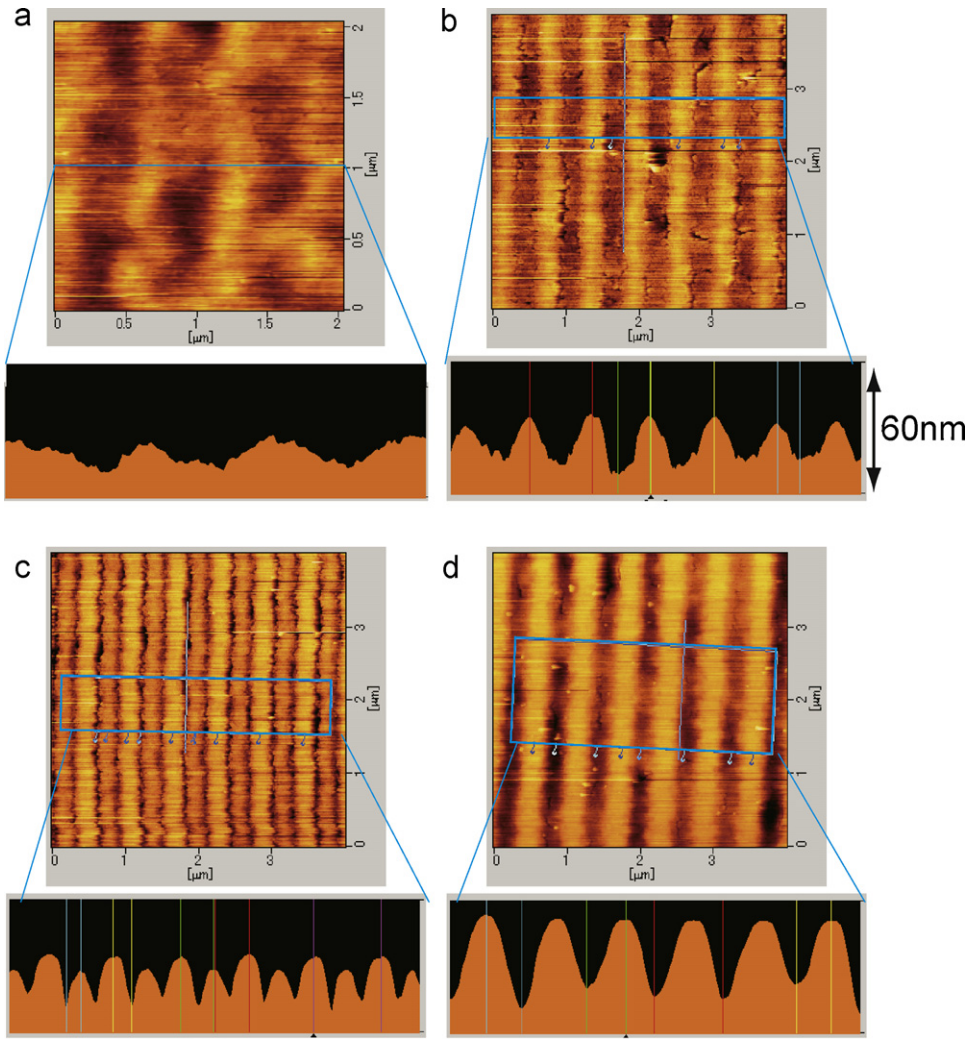

Fig. 5. AFM images of the surfaces of TiO_2-organic hybrid films prepared by irradiation for (a) 5 min by a mask A, (b) 3 min, (c) 5 min, and (d) 7 min by a mask B.

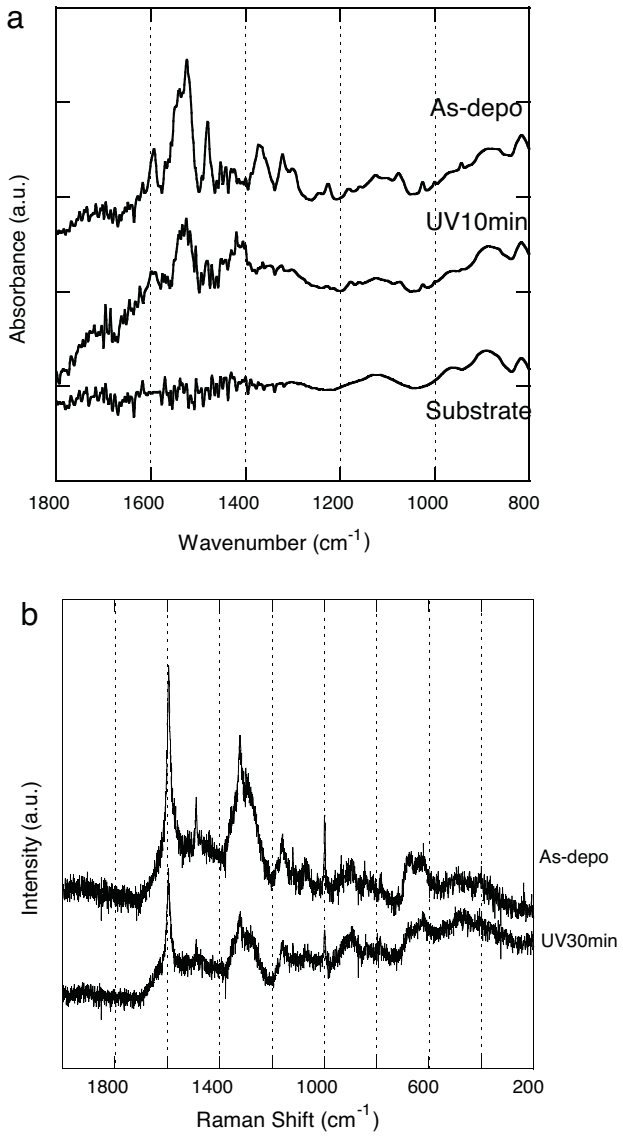

Fig. 7. (a) IR spectra and (b) Raman spectra of the TiO_2-organic hybrid film before and after UV irradiation.

3. Experimental details

A TiO_2-organic hybrid gel film was prepared by the sol–gel method according to a previous report [12]. Titanium tetra-n-butoxide ($Ti(O\text{-}nBu)_4$, Soekawa Chemical Co., Ltd.) was allowed to react with dibenzoylmethane (DBM, Wako Pure Chemical Ind., Ltd.) and methacrylic acid (MA, Wako Pure Chemical Ind., Ltd.) in 2-ethoxyethanol (Wako Pure Chemical Ind., Ltd.). The molar ratio of $Ti(O\text{-}nBu)_4$, DBM, MA, and 2-ethoxyethanol was 1:1:1:20. Half of the volume of the 2-ethoxyethanol was first used as a solvent for the mixture of $Ti(O\text{-}nBu)_4$, DBM, and MA. After the solution was stirred for 15 min at room temperature, a mixture of H_2O and the remaining 2-ethoxyethanol was dropped into the sol. The molar ratio of H_2O to $Ti(O\text{-}nBu)_4$ was 4:1. The sol was stirred for 3 h at room temperature, and was spin-coated at 5000 rpm for 30 s on a glass substrate. The film thickness was approximately 300 nm.

Line and space patterns of Al were fabricated by electron beam lithography and dry etching techniques. Two types of Al films with a thickness of 30 nm were coated on silica glasses, and AFM images of the surface of the Al are shown in Fig. 3; (a) the arithmetic averages of the roughness were Ra = 2.5 nm and (b) Ra = 0.59 nm.

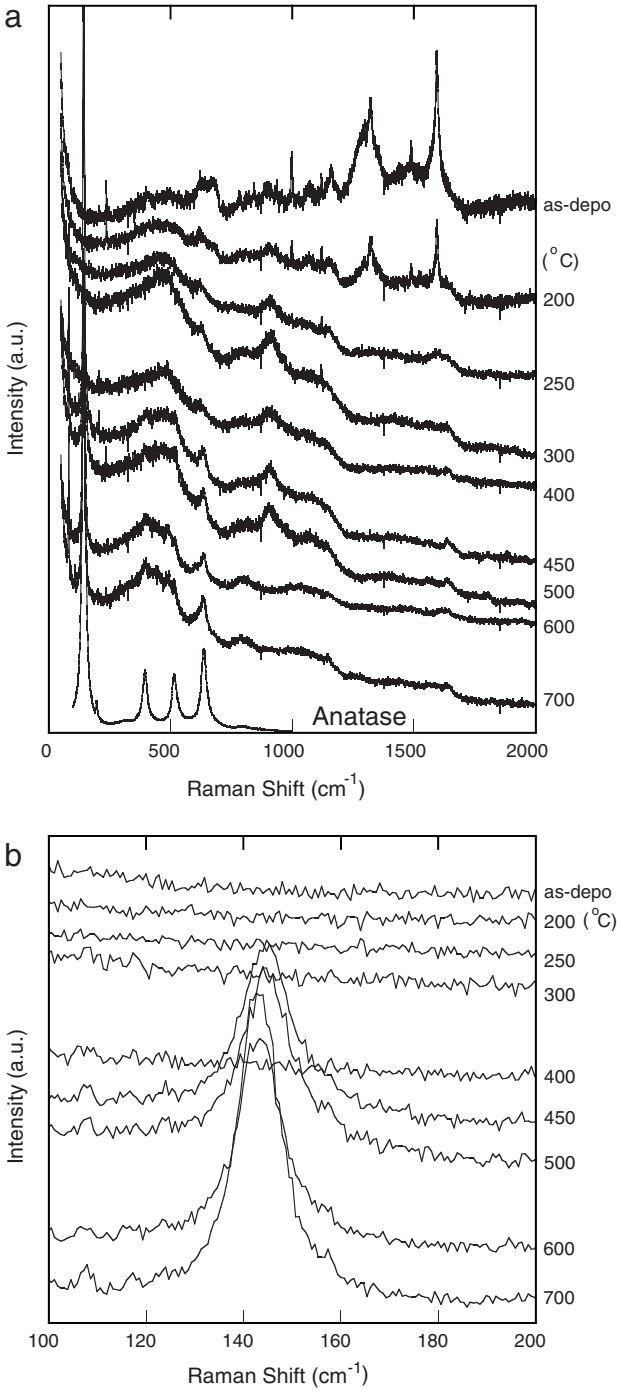

Fig. 8. Raman spectra of the TiO_2-organic hybrid film heated at different temperatures for 1 h. (b) is expanded (a) in the range from 100 to 200 cm^{-1}.

Patterns in which the line width was 500 nm and spaces between neighboring lines were 90 nm were prepared based on the FDTD calculation results. A resist (ZEP-520A, Zeon Co., Ltd.) was coated on the Al, and patterns were drawn by electron-beam lithography (Elionix, ELS-7500EX). The reacted parts were removed in ZED-N50 and rinsed with ZMD-B. The Al films were etched by an ICP-RIE (CE-300I, Ulvac). After the dry-etching, the resist film was removed by dipping in dimethylacetamide followed by oxygen plasma ashing, resulting in Al patterns. The patterns prepared by each Al thin film were referred to as mask A and mask B, respectively. A SEM image of the Al pattern of mask B is shown in Fig. 4. The dark parts are Al, and the lighter parts represent the surface of the silica glass. It was

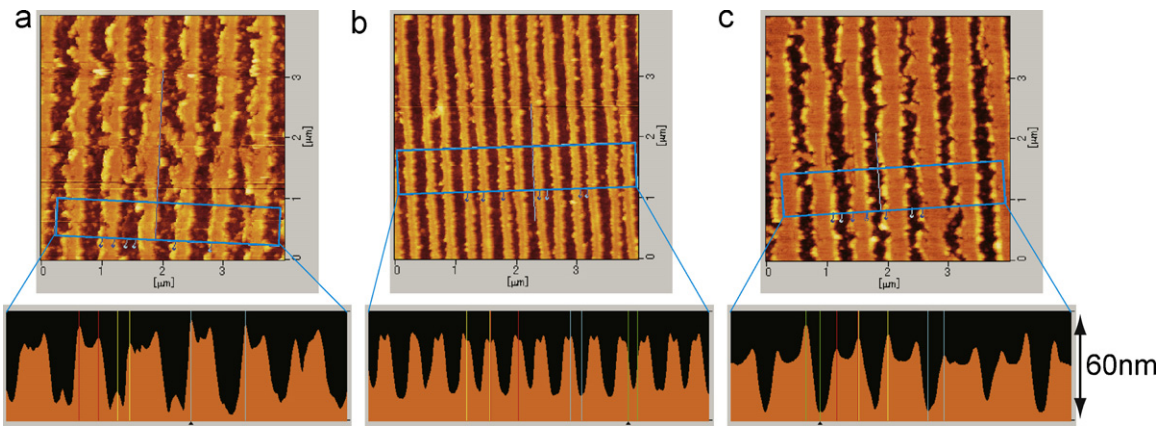

Fig. 9. AFM images of the surfaces of TiO_2 films prepared by irradiation for (a) 3 min, (b) 5 min, and (c) 7 min, and heated at 500 °C.

confirmed that the Al patterns of both Al masks were smooth and straight.

The coated hybrid film was baked at 80 °C for 10 min. After baking, the Al mask was placed in contact with the hybrid films and irradiated with UV light (Sanei electric., SUPERCURE-204S) at 290 mW/cm^2 for several minutes through the mask. After the UV irradiation, the unreacted parts of the films were removed by iso-propanol. The surfaces of the nano-patterns were evaluated by atomic force microscope (AFM, SII, L-trace).

The films before and after UV irradiations were measured to investigate the chemical reactions by UV–vis, IR, and Raman spectra. UV–vis spectra were measured at the irradiated area in a square 200 μm on a side on the film coated on a silica glass by UV–vis spectrometer (JASCO, MSV-370). The IR spectra of the film coated on a silicon substrate were measured before and after UV irradiation by IR spectrometer (Perkin Elmer, SPECTRUM GX 2000R). The Raman spectra of the surface of the film before and after UV irradiation and the films after heating for 1 h were measured to investigate the changes from the hybrid film to TiO_2 film, as follows. Raman measurements were performed in a backward micro-configuration, using the 514.5-nm line from an Ar^+ laser (1 mW) focused to a 1 μm-diameter spot on the crystal surface. The scattered light was dispersed by a subtractive triple spectrometer (Horiba-Jobin Yvon, T64000) and collected with a liquid-nitrogen-cooled charge-coupled device (CCD) detector.

4. Results

Fig. 5 shows AFM images of the surface of the prepared patterns. Fig. 5(a) shows the AFM image of the pattern prepared by irradiation for 5 min using mask A. Fig. 5(b)–(d) shows the AFM images of the patterns prepared using mask B by irradiation for (b) 3 min, (c) 5 min, and (d) 7 min. In Fig. 5(a), the patterns were slightly convex with a pitch of approximately 600 nm, which corresponded to the distance between the neighboring Al lines. However, the line and space patterns were not clear and straight, meaning that the photoreaction was not sufficient to make patterns. In Fig. 5(b) and (d), the surface was convex with a pitch of approximately 600 nm. The height of the convex surface prepared by 3-min irradiation was approximately 25 nm, and lower than that obtained under the 7-min irradiation; 40-nm. In Fig. 5(c), the surface is convex with a pitch of approximately 300 nm. The height of the convex surface was approximately 15–20 nm.

Fig. 6 shows UV–vis transmittance spectra of the hybrid film before and after irradiation with UV light for 5 min. The spectra had a valley at around 400 nm, which is assigned to a π–π^* transition of the chelate ring formed by the reaction between ketone in DBM and Ti alkoxide [12]. The valley became small after irradiation with UV light. The changes mean that the chelate was decomposed by UV irradiation for 5 min. Fig. 7(a) shows IR spectra before and after irradiation of UV for 10 min. Fig. 7(b) shows Raman spectra before and after UV irradiation for 30 min. Based on comparison with these spectra, the peak at around 1600 cm^{-1} was assigned to the vibration of C=C bonds. The peak intensity decreased after UV irradiation. From these changes in both the IR and Raman spectra before and after UV irradiation, it was found that the C=C bonds in methacrylic acid were photopolymerized due to the radicals that were generated from DBM by UV irradiation. The structural changes in chelate compounds and the photopolymerization of methacrylic acid should cause a decrease in the solubility into iso-propanol of the photoreacted parts.

Fig. 8 shows Raman spectra of the hybrid films after heating at different temperatures. The as-deposition film and that heated at 200 °C had many peaks at around 1000–1800 cm^{-1}, which were assigned to organic groups. The strong peaks at around 1600 cm^{-1} and 1300 cm^{-1} were assigned to symmetry C=C and C–C bonds, respectively, and they disappeared in response to heating at a temperature above 250 °C. This means that the main bonds of the DBM and MA were decomposed by the heating at temperatures above 250 °C. On the other hand, a broad peak was observed at around 800 cm^{-1} in the spectra of films heated from 200 to 500 °C. The peak would be assigned to the vibration of C–H in the remaining organic compounds such as phenyl groups. The Raman spectrum of anatase is shown as a reference in Fig. 8(a). The typical vibration peaks of anatase appear at 140, 400, 550, and 700 cm^{-1}. The peak at 700 cm^{-1} became sharp in response to heating over 450 °C. In Fig. 8(a), the strongest peak at around 140 cm^{-1} cannot see well. Thus, the region from 100 to 200 cm^{-1} is extended in Fig. 8(b). The peak assigned to anatase appeared for the films heated to over 450 °C, meaning that anatase can be formed by heating to over 450 °C, although small quantities of some organic compounds remained in the film.

The obtained patterns, as shown in Figs. 5(b)–(d), were heated at 500 °C, and the AFM images are shown in Fig. 9. In Fig. 9, the UV irradiation times for the photoreactions were (a) 3 min, (b) 5 min, and (c) 7 min. The pattern heights increased compared with those before heating. From the Raman spectra, as shown in Fig. 8, almost all of the organic compounds were removed and the TiO_2 remained. The pitch of center of the patterns prepared by 3-min and 7-min irradiation was approximately 600 nm, and corresponded to that before heating. The edges of each convex pattern were higher than the center and looked like peaks, and the pitch of the peaks at each edge was approximately 300 nm. The patterns prepared by 5-min irradiation had more convex patterns, and the distance between the neighboring patterns was approximately 300 nm, which corresponded to half of the pitch of the Al mask.

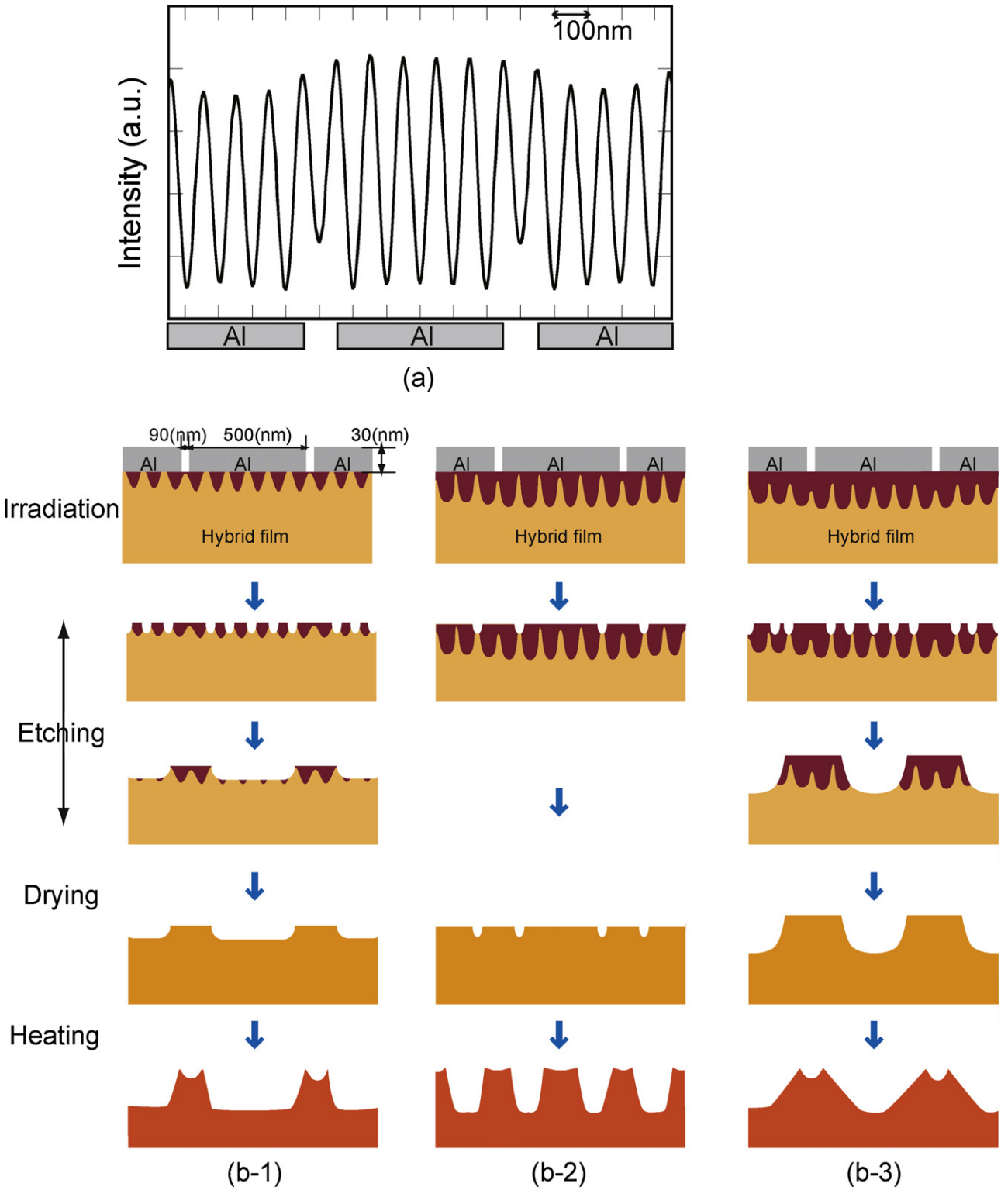

Fig. 10. (a) Calculated intensity of the electric field of the 10 nm below the Al surface. (b) Schematic models during the chemical reaction and heating of the irradiation for (b-1) 3 min, (b-2) 5 min, and (b-3) 7 min.

5. Discussion

From the UV–vis, IR, and Raman spectra, it was confirmed that the hybrid film was photoreacted by the irradiation of UV light, that chelate rings formed by Ti alkoxide and DBM were decomposed, and that the C=C bonds in the methacrylic acids were photopolymerized. The line and space patterns were obtained when the mask B with a flat surface was used. Taking the FDTD calculations, as shown in Fig. 2, into account, the enhancement of the SP on the rough Al film was weaker than that on the flat Al. Based on comparison with the patterns prepared by masks A and B, it was found that the patterns depended on the intensity of the SP enhance-

ment. These results indicate that the patterns were obtained by the SP enhancement. However, the pitch of the convex patterns was approximately 300 nm or 600 nm, which did not correspond to the calculated interfering electric distribution, approximately 100 nm. Thus, the relationship between the chemical reaction and the obtained patterns has been discussed follows.

Fig. 10(a) shows the calculated electric field intensity below 10 nm under the Al film as a typical intensity distribution of the SP. The calculated electric field is shown in Fig. 1(b); the distribution of the enhancement shows little dependence on the distance from the Al surface, although the intensity decreased with increased distance from the surface. The intensity of the SP had peaks with approximately 100-nm pitch, and the SP around the slits of the Al was slightly stronger than the surface of the Al. Fig. 10(b) shows schematic models during the chemical reaction and heating. Fig. 10(b-1), (b-2), and (b-3) shows the models prepared by irradiation for 3 min, 5 min, and 7 min, respectively. The hybrid films were photoreacted (the photoreacted regions are shown in red in Fig. 10(b)), and the regions were extended with increases in the irradiation time. Generally, the unreacted regions in the hybrid films were removed in alcohol [12]. The unreacted and nonsufficiently reacted regions were removed when the photoreacted films were etched. The hybrid films under the slits of Al were photoreacted slightly better than the other regions, resulting in the regions around the slits remaining. In the case of 5-min irradiation, the center region under the Al also remained. Thus, the patterns with 300-nm or 600-nm pitch were obtained after drying. After heating, the patterns were convex around the edge, as shown in Fig. 9, which may indicate that the TiO_2 networks were formed more at the edges than the center, which corresponded to the photoreacted regions. These results might suggest that the etching time is sufficient to remove not only the unreacted regions but also the reacted regions. Thus, patterns with approximately 100 nm pitch might be obtained by the interference of the SP, if the UV irradiation and etching time are optimized more strictly.

6. Conclusions

In summary, the TiO_2-organic hybrid materials were patterned with nanometer size by interference of the surface plasmon of Al. The chelate rings of the TiO_2-organic hybrid materials were decomposed, and the C=C double bonds were photopolymerized by the surface plasmon enhanced by the irradiation of UV light. The TiO_2-organic hybrid materials changed to anatase by sintering at temperatures above 450 °C. The photopolymerization of the inorganic–organic hybrid materials induced by the SP can be applicable to nano-patterning of ceramics.

Acknowledgements

This work was supported by funding from the Ministry of Education, Culture, Sports, Science, and Technology of Japan: KAKENHI Grant-in-Aid (No. 21020013) for Scientific Research of the Priority Area “Strong Photon-Molecule Coupling Field for Chemical Reactions” (No. 470). The patterning of the Al was supported by the MANA Foundry in the National Institute for Materials Science.

References

[1] J. Aizenberg, J.A. Rogers, K.E. Paul, G.M. Whitesides, Appl. Phys. Lett. 71 (1997) 3773–3775.
[2] J.G. Goodberlet, H. Karvak, Appl. Phys. Lett. 81 (2002) 1315–1317.
[3] M. Naya, I. Tsuruma, T. Tani, A. Mukai, S. Sakaguchi, S. Yasunami, Appl. Phys. Lett. 86 (2005) 201113.
[4] M.A. McCord, J. Vac. Sci. Technol. B 15 (1997) 2125–2129.
[5] J.P. Silverman, J. Vac. Sci. Technol. B 16 (1998) 3137–3141.
[6] S.Y. Cho, P.R. Krauss, P.J. Renstrom, Science 272 (1995) 85–87.
[7] X. Luo, T. Ishihara, Appl. Phys. Lett. 82 (2004) 4780–4782.
[8] H. Raether, Surface plasma oscillations and their applications, in: G. Hass, M.H. Francombe, R.W. Hoffman (Eds.), Physics of Thin Films, Academic Press Inc. Ltd., 1977, pp. 145–261.
[9] D.Y. Smith, E. Shiles, M. Inokuti, The optical properties of metallic aluminum, in: E.D. Palik (Ed.), Handbook of Optical Constants of Solids, Academic Press Inc. Ltd., 1985, pp. 369–406.
[10] Y. Ekinci, H.H. Solak, J.F. Loffler, J. Appl. Phys. 104 (2008) 083107.
[11] W. Srituravanich, N. Fang, C. Sun, Q. Luo, X. Zhang, Nano Lett. 4 (2004) 1085–1088.
[12] H. Segawa, S. Adachi, Y. Arai, K. Yoshida, J. Am. Ceram. Soc. 86 (2003) 761–764.
[13] H. Segawa, N. Abrams, T.E. Mallouk, I. Divliansky, T.S. Mayer, J. Am. Ceram. Soc. 89 (2006) 3507–3511.